


Article

Preparation and fluorescent wavelength control of multi-color Nitrogen-doped carbon nano-dots

Wenli Li^{1,†}, Ju Tang^{1,2,†}, Yuzhao Li¹, Han Bai¹, Weizuo Zhang¹, Jin Zhang^{1,3,*}, Yiming Xiao^{1,*} , and Wen Xu^{1,4,5,*}

¹ School of Physics and Astronomy, Yunnan University, Kunming 650091, China; 18388308185@163.com (W.L.); jutang_ynu@163.com (J.T.); liyuzhao@mail.ynu.edu.cn (Y.L.); bh001925@163.com (H.B.); zhangwz@ynu.edu.cn (W.Z.)

² Department of Physics, School of Electrical and Information Technology, Yunnan Minzu University, Kunming 650504, China

³ Yunnan Carbon Base Technology Co. LTD, Kunming 650028, China

⁴ Micro Optical Instruments Inc., 518118 Shenzhen, China

⁵ Key Laboratory of Materials Physics, Institute of Solid State Physics, HFIPS, Chinese Academy of Sciences, Hefei 230031, China

* Correspondence: zhangjin@ynu.edu.cn; yiming.xiao@ynu.edu.cn; wenxu_issp@aliyun.com

† These authors contributed equally to this work.

Version November 30, 2021 submitted to Nanomaterials



Abstract: It is known that, by taking advantage of heteroatom doping, the electronic states and transition channels in carbon nano-dots (CNDs) can be effectively modulated. Thus, the photoluminescence (PL) properties of CNDs can be changed. For potential applications of CNDs as advanced materials for optoelectronic devices, it is important and significant to develop the practical techniques for doping heteroatoms into CNDs. In this work, we synthesize the multi-color fluorescent by using a fast and effective microwave method where the CNDs are nitrogen-doped. We examine the influence of different ratios of the raw materials on the structure and optical properties of N-CNDs. The results show that the prepared N-CNDs can generate blue (445 nm), green (546 nm), and orange (617 nm) fluorescence or PL with the mass ratio of the raw materials at 1:1, 1:2 and 1:3, respectively. We find that the N content in N-CNDs leads to different surface/edge states in $n - \pi^*$ domain. Thus, the wavelength of the PL emission from N-CNDs can be tuned via controlling the N concentration doped into the CNDs. Moreover, it is shown that the intensity of the PL from N-CNDs is mainly positively related to the content of C-O groups attached on the surface/edges of the N-CNDs. This study provides an effective experimental method and technical way to improve the fluorescent emission, and to modulate the color of the PL emission from CNDs.

Keywords: carbon nano-dots; nitrogen doping; fluorescence wavelength regulating

1. Introduction

Carbon nano-dots (CNDs) are new types of carbon-based nanomaterials [1,2]. The structure of CNDs is generally considered to be composed of sp_2/sp_3 carbon and oxygen/nitrogen based-groups or polymer groups [3]. This means that CNDs have better practical applications in many fields, such as light-emitting devices, biological imaging, photothermal therapy, photocatalysis, electrochemical energy

storage, biomedical [4] and visual precision pH sensing [5]. In particular, due to the flexibility of surface modification and the tunable PL emission wavelength, CNDs have gradually become the most suitable alternative material for the application of metal nanoclusters and traditional dye molecules in the field of optoelectronics [6].

Due to the structural differences caused by different raw materials and experimental conditions, CND systems often have different PL emission behaviors. In general, the PL properties of CNDs depend strongly on the carbon source, synthesis technology, parameter setting in the preparation process, and edge/surface modulation [7,8]. More specifically, the intensity and frequency positions of PL emission of CNDs are subject to the existence of different functional groups or edge states, the interaction between the electronic states of sp_2 conjugated domain, the interaction between the electronic states in surface state chemical groups/hanging bonds, and the properties of fluorophores in CNDs [9,10]. However, there is no final conclusion on the photoluminescence mechanism of CNDs. It is generally believed that the photoluminescence mechanism of CNDs depends on quantum confinement effect [11], surface state [12–17], and molecular state [18]. It is worth noting that the existence of surface/defect states is the potential reason for the PL excitation dependent luminescence characteristics. The fluorescence of surface/defect states as PL emission centers can be generated directly by optical pumping excitation, or by the energy transfer of eigenstates [19,20]. Therefore, the preparation of tunable fluorescent CNDs and the disclosure of its optical mechanism are particularly important.

Recently, the effect of the pH values on fluorescence properties of CNDs has also been investigated [5,21,22]. Wang et al. [18] reported that the reflux of a solution containing L-cysteine and galactose with NaOH at different concentrations can emit PL with different colors. The PL wavelength generated from CNDs would be shorter with increasing NaOH concentration. By the way, temperature also plays an important role in carbon precursor carbonization or cutting up carbon/graphite materials for the preparation of CNDs. Reaction temperature during the synthesizing of CNDs can affect the chemical, physical and bio properties of CNDs, such as the degree of carbonization or crystallization, particle size, types of surface/edge functional groups, the corresponding PL strength, and peak position [19, 20]. Generally, with increasing reaction temperature, it can gradually increase the contents of special hetero-atoms or produce a new molecular structure in the preparation of CNDs [23]. For example, the preparation of nitrogen-doped CNDs at high temperatures 600–900 °C can form a variety of molecular structures in the carbon structure, such as pyridine, pyrrole or graphite nitrogen [24]. It has been noticed that the synthesis method can also affect the wavelength of the PL emission from CNDs prepared with the same initial precursor [25]. The emission spectra of carbon dots dependent on the excitation wavelength for most cases and only exhibit excitation-independent behavior when CNDs were fully surface-passivated [26,27]. Typically, the structure of citric acid (CA) contains multiple hydroxyl and carboxyl groups, and it is one of the most commonly used precursors for carbon dots preparation by a bottom-up method [26]. If CA and urea are used as precursors, by varying the mole ratio of CA/urea and the reaction temperature, the carbon dots can emit blue to red light, covering the entire light spectrum. When the reaction temperature is at 200 °C and the mole ratio of CA/urea is greater than 0.7, red carbon dots with the maximum emission peak at 630 nm have the fluorescence quantum efficiency of 12.9%. It suggests that temperature and mole ratios of CA/urea can tune the maximum emission of carbon dots from blue–green to red [27]. Inspired by the above research, we propose a simpler and more environmentally friendly method to prepare CNDs with adjustable luminous intensity and wavelength. In this work, we use the citric acid and L-glutamic acid as carbon resources to fabricate the CNDs. By controlling the ratio between citric acid and L-glutamic acid, the multi-color N-CNDs can be obtained in deionized water as a dispersing agent. From a viewpoint of material application, it is important and significant to understand and to examine the dependence of the intensity and wavelength of the PL emission from CNDs on the ratio of the raw materials. This becomes the prime motivation of the present study.

2. Experiment

2.1. Raw Materials

The analytically pure citric acid and L-glutamic acid were purchased from Afisa Chemical Limited Liability Company (Tianjin, China). The deionized water was produced in the laboratory.

2.2. Preparation of N-CNDs by Means of Microwave and Experimental Measurements

The general processes to synthesize the CNDs from citric acid and L-glutamic acid are as follows: (i) Citric acid and L-glutamic acid were mixed evenly with the mass ratio at 1:1 (1 g:1 g), 1:2 (1 g:2 g) and 1:3 (1 g:3 g), respectively. Here, the mixture is put into the beaker and placed into the microwave for constant heating. (ii) After being clarified and fully reacted in a microwave reactor for 5 min, the microwave heating temperature is 300 degrees Celsius, and the power is 800 watts. (iii) We let the stuff in the beaker cool down naturally till room temperature and add 10 mL deionized water into the beaker. (iv) The mixture is magnetically stirred for 10 min to achieve the uniform and full mix of the matters and water. The mixture is further centrifuged at a speed of 12,000 r/min for 30 min. After purifying by the dialysis bag (the aperture is 30,000 D), we can obtain the solutions which contain CNDs. The diagram of the preparation procedure of CNDs is shown in Figure 1. We obtain the N-CNDs, which can emit blue, green and red fluorescent light, respectively.

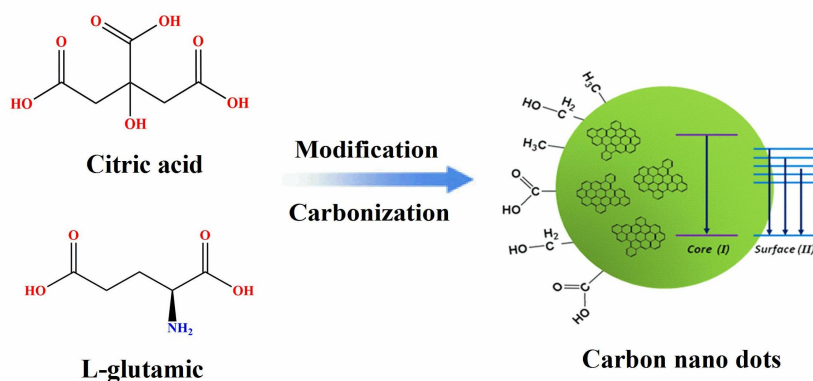


Figure 1. The diagram of the preparation procedure of CNDs.

The PL spectra of N-CNDs solutions were measured by a fluorescence spectrometer F9818012 (SHANGHAI LENGGUANG TECHNOLOGY CO., LTD, Shanghai, China). The X-ray photoelectron spectroscopy (XPS) of N-CNDs was measured by using PHI5000 Versa Probe II photoelectron spectrometer (Thermo Scientific, New York, NY, USA) with Al K_{α} at 1486.6 eV. The morphology and micro-structures of the CNDs were characterized by using the JEM 2100 transmission electron microscopy (JEOL, Tokyo, Japan), with an accelerating voltage of 300 kV. The Fourier-transform infrared (FT-IR) spectra of the CNDs were recorded on a Perkin Elmer TV1900 instrument (Thermo Scientific, New York, NY, USA). The UV-Vis absorption spectra were measured by a Specord 200 UV-Vis spectrophotometer (Germany Jena (Zeiss) Co., Jena, Germany).

3. Results and Discussions

In Figure 2, we show the TEM images of morphology and lattice stripes (the inserted image, HRTEM image) of N-CNDs, and particle size distribution (the inserted chart) of CNDs. Here, the N-CNDs were

fabricated by mixing citric acid with L-glutamic acid at the ratio of 1:3. We can see that N-CNDs are with clear crystal structures and their morphology is disk-like. The size of CNDs is in the range of 1.5–4.0 nm, with an average size of 2.6 nm. From the HRTEM image of single N-CND (see lower inset), the well-resolved lattice fringes with inter-planar spacing of 0.216 nm were obtained. This value is close to the (100) diffraction facets of graphite carbon, which indicates that the carbon core of the N-CNDs is with good crystallinity [28].

Figure 3a–c shows the fluorescence emission spectra of blue-CNDs (B-CNDs), green-CNDs (G-CNDs), and orange-CNDs (O-CNDs) prepared by the mixture of citric acid and L-glutamic acid, with the ratio of 1:1, 1:2 and 1:3, respectively. When B-CNDs, G-CNDs, and O-CNDs are excited by the wavelengths of 360 nm, 470 nm and 530 nm, the corresponding peak position of fluorescence emissions from B-CNDs, G-CNDs, and O-CNDs are located at wavelength of 445 nm, 546 nm, and 617 nm, respectively. The fluorescence intensity of them are increasing with increasing of excitation wavelength for three types of CNDs. The peak positions of PL for these CNDs are slightly shift with different excitation wavelengths. During the PL measurement, the influence of UV exposure on the PL intensity of the B-CNDs, G-CNDs, and O-CNDs had also been examined. The PL intensity does not vary under continuous UV irradiation for hours for B-CNDs, G-CNDs, and O-CNDs in deionized water. This indicates that the CNDs prepared are quite stable and would have good photostability for the practical applications. The results imply that the fluorescence properties induced by N impurity in these N-CNDs are quite stable. Furthermore, in Figure 4, we show the chromaticity diagrams of N-CNDs, with different raw ratios at optimal excitation wavelengths. The color coordinates shown in the chromaticity diagram indicate that the B-CNDs, G-CNDs, and O-CNDs excited with the optimal excitation wavelength can emit blue, green, and orange light, respectively.

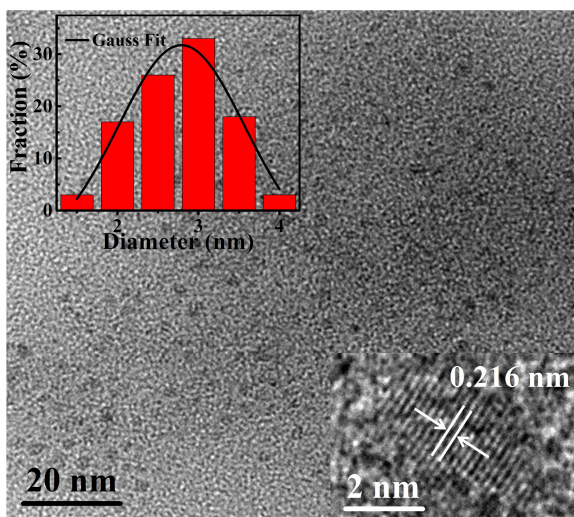


Figure 2. TEM images of N-CNDs, their lattice fringes (HRTEM image, lower inset), and the diameter distribution (upper inset).

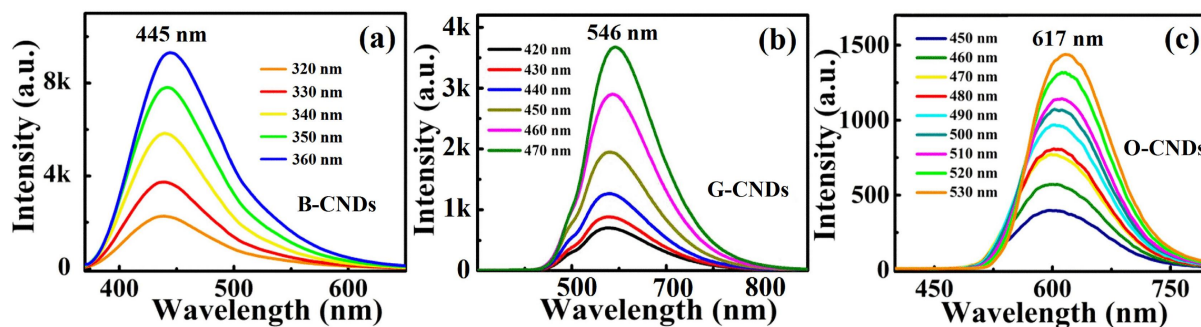


Figure 3. The PL spectra of (a) B-CNDs, (b) G-CNDs, and (c) O-CNDs prepared by the mixture of citric acid and L-glutamic acid with the mass ratio of 1:1, 1:2, and 1:3, respectively.

The quantum yield Q of B-CNDs, G-CNDs and O-CNDs can be evaluated from the experimental data via [29]

$$Q = Q_S \cdot \frac{I_S}{I} \cdot \frac{A}{A_S} \cdot \frac{\eta}{\eta_S}, \quad (1)$$

where Q_S is the quantum yield of the fluorescence for a standard sample for reference. Under a fixed excitation wavelength at, e.g., 360 nm, 470 nm and 530 nm. I and I_S are the integrated emission intensities of the CNDs sample and the standard sample, respectively. A and A_S are respectively the absorbance of the prepared sample and standard sample at the same excitation wavelength. η and η_S are respectively the refractivity of the prepared sample and standard sample. The standard sample of B-CNDs is quinine sulfate; the standard sample of G-CNDs and O-CNDs is rhodamine. It is found that the fluorescent quantum yield of B-CNDs, G-CNDs and O-CNDs is about 21.37%, 16.12% and 9.11%, respectively.

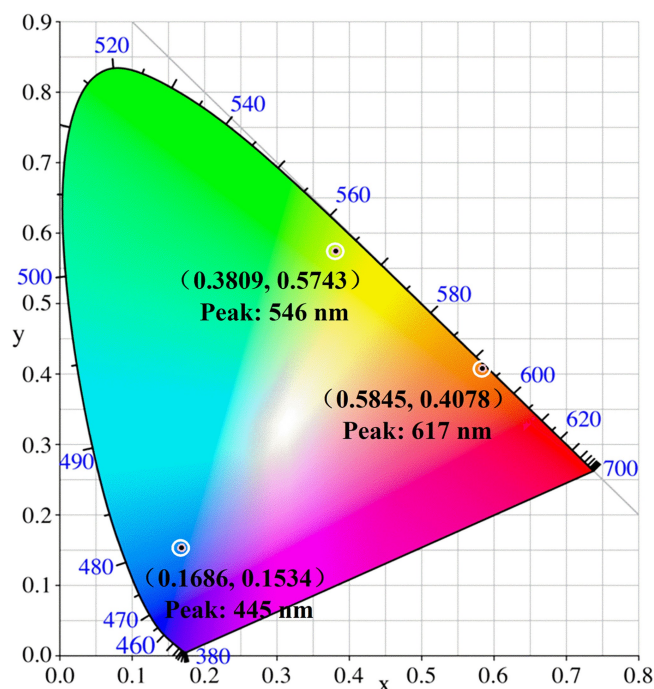


Figure 4. The chromaticity diagrams of N-CNDs with different raw ratios at optimal excitation wavelength.

The XPS spectra and peak fitting diagrams of N-CNDs prepared by citric acid and L-glutamic acid are shown in Figure 5 with the ratios of 1:1, 1:2, and 1:3. The XPS spectra have three peaks at 285 eV, 399 eV, and 532 eV, which correspond to C1s, N1s, and O1s peaks of the N-CNDs, respectively. The results reveal that three N-CNDs samples are composed of C, N and O elements, and the concentrations of these elements in B-CNDs, G-CNDs, and O-CNDs were different. We can see that the nitrogen content increases with increasing the ratio of citric acid to L-glutamic acid. In Figure 5(a1–c1), it is worth noting that the fluorescence wavelengths of N-CNDs show a red shift with the increase of the N doping concentration. By comparing Figures 3a–c and 5(a4–c4), it can be found that the fluorescence intensity of N-CNDs is decreasing with decreasing the C–O groups on the surface of N-CNDs.

However, the actual mechanism of fluorescence emission from CNDs is not clear [3]. It has been shown that the surface defects caused by surface oxidation (C=O and C–O groups attached to CNDs) can be used as the capture center of exciton, which could result in fluorescence emitting from CNDs [30]. The elemental analysis in Figure 5(a1–c1) shows that the contents of N in B-CNDs, G-CNDs, and O-CNDs samples are 3.6%, 3.75%, 4.21%, which increase regularly with increasing the ratio between citric acid and L-glutamic acid. The N doping elements in CNDs shown in Figure 5(a2–c3) could also be the exciton capture centers which can change the surface state of CNDs and lead to fluorescence similar to C=O and C–O groups [28,31,32].

The deconvolution of high-resolution C1s XPS spectra in Figure 5(a2–c2) reveals peaks at 284.8 eV, 286.4 eV, and 288.2 eV, which correspond respectively to C–C/C=C, C–N/C–O, and C=O/C=N bonding in N-CNDs [33]. The stronger peak of C–C/C=C indicates the better lattice structure of the sp^2 carbon (C–C/C=C) area. The high-resolution spectra of N1s for N-CNDs in Figure 5(a3–c3) contains Pyridinic N (398.5 eV), Amino N (399.4 eV), Pyrrolic N (400.2 eV), and Graphite N (401.0 eV) [34,35]. It is shown that a trace of nitrogen atoms enters the carbon nucleus of N-CNDs and forms the PL luminous center of N-CNDs through the hybrid of edge groups with carbon nucleus [36]. The high-resolution spectra of

O1s in Figure 5(a4–c4) for N-CNDs contain C=O (531.1 eV) and C-O (C-O-C/C-OH) (532.7 eV) [35,37]. The quantity decreasing of C-O (C-O-C/C-OH) from a4 to c4 in Figure 5 is consistent with reducing the fluorescence intensity in Figure 3a–c. The intensity of PL emission changes with the peak's position of C-O (C-O-C/C-OH). The intensity of the PL emission increases with increasing the peak height of C-O (C-OH), and with reducing the peak height of O-C=O. This is in line with the result we obtained previously [38]. Therefore, it's reasonable to believe that B/G/O-CNDs have various edge groups, such as C-OH, C-N, C=O, and C-H. These edge groups can induce different kinds of surface states and influence the intensity of PL spectra.

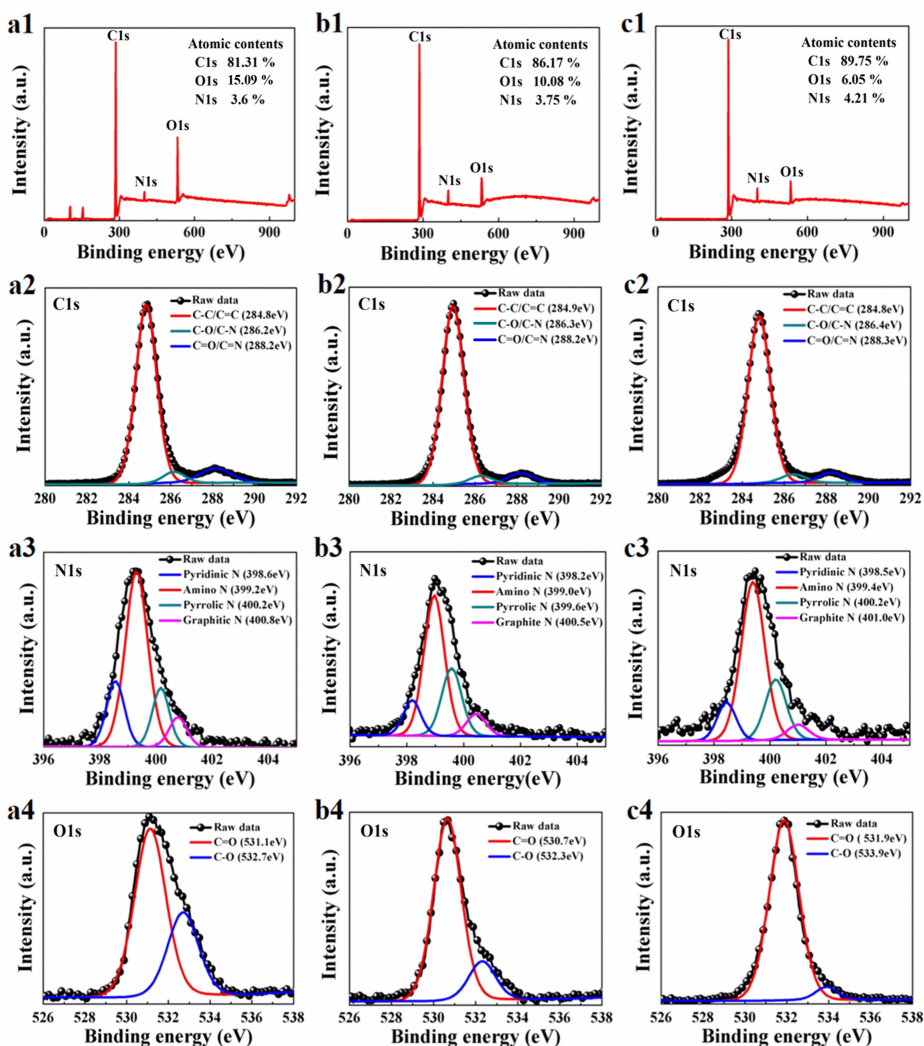


Figure 5. The full-scan XPS spectra in (a1–c1), the high-resolution spectra of C1s in (a2–c2), N1s in (a3–c3), and O1s in (a4–c4) for B-CNDs, G-CNDs, and O-CNDs, respectively.

The above results show that N-doping has effects on the light emission of CNDs. As can be seen from Figure 6a, the absorption peak of B-CNDs and G-CNDs is at 358 nm, and a clear absorption peak at 302 nm is observed for O-CNDs. These absorption peaks are attributed by the functional group (C=O) on the surface of N-CNDs [39]. These N-CNDs have different surface states, and the light emissions may originate from the radiation recombination of the excited electrons [40]. Thus, the PL emission properties

of N-CNDs is mainly attributed to the N-doping effect. The surface groups of N-CNDs prepared under microwave conditions were analyzed by FT-IR [41] and shown in Figure 6b. It can be shown that the stretching vibrations of O-H are at $3400\text{--}3200\text{ cm}^{-1}$, which indicates that N-CNDs are rich in hydroxyl groups. The characteristic absorption frequency of C=O ($1600\text{--}1900\text{ cm}^{-1}$) near 1646 cm^{-1} overlaps with that of C=C/C-C ($1500\text{--}1675\text{ cm}^{-1}$). We can understand that there are carboxy groups around the carbon spot. The vibration absorption peak of N-C₃ is at 2063 cm^{-1} . The absorption peak of C-O bond stretching vibration is at 1401 cm^{-1} , and this is the evidence of the polymerization between citric acid or L-glutamic acid. The bending vibration absorption peak of C-N is at 1231 cm^{-1} and the absorption peak of C-O-C is at 1045 cm^{-1} . The results in Figure 6 imply that the particles are surrounded by functional groups, such as hydroxyl groups and carboxy groups. These functional groups not only improve the water solubility and biocompatibility of N-CNDs, but also contribute to the surface modification of N-CNDs. These are in good agreement with the results obtained from XPS spectra.

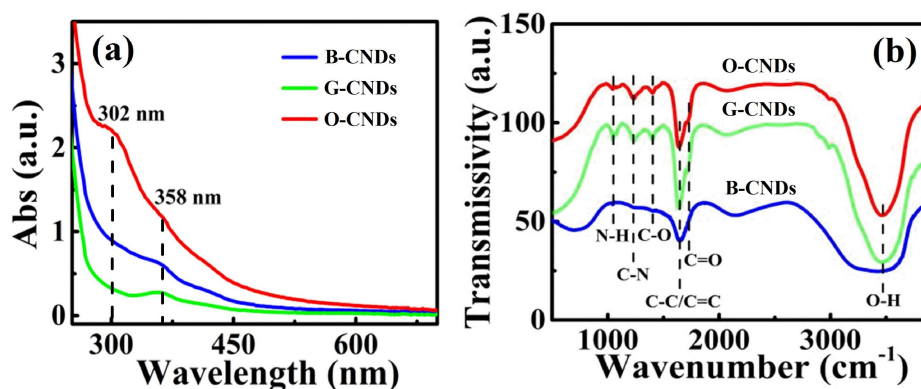


Figure 6. UV-vis (a) and FT-IR (b) absorption spectra for N-CNDs.

Figure 7 shows the color tuning mechanism of N-CNDs. With increasing the N doping concentration of N-CNDs, more surface states are introduced, and the lowest energy level of surface states decreases [20]. The fluorescence wavelength of N-CNDs would have red-shifts. As a result, the fluorescence wavelengths of N-CNDs can be tuned through controlling N-doping concentrations of N-CNDs. Multitudinous surface states on N-CNDs result in a wide range of energy bands, which correspond to broad absorption bandwidths and the excitation wavelength-dependent emission spectra. From the viewpoint of physics, CNDs have strictly discrete electron energy levels, and the filling distribution of electrons determines the molecular states. The molecular states are divided into singlet and triplet states. At room temperature, most of the bonding electrons in the molecules of fluorescent substances are in the ground state. Under the action of optical shining, some of the bonding electrons in the ground state move to a higher electron excited state, resulting in the phenomenon of molecular absorption in spectrophotometry. The electrons at the excited state energy level are in the non-ionized state. The electrons in the first excited state can transition to the second excited state, through non radiative transitions such as internal conversion and vibrational relaxation. In the process of decaying back to each vibrational level in the ground state, they release energy or photons and produce fluorescence.

As can be seen, the surface of N-CNDs prepared in the work contains a large number of functional groups, which can make N-CNDs show a strong affinity for biomass. Therefore, N-CNDs can be dispersed and adsorbed on biomass materials, such as paper plates and clothing walls, which can emit bright fluorescence under UV light excitation. Therefore, N-CNDs would have potential application value in interior decoration, anti-counterfeiting trademark, and other fields.

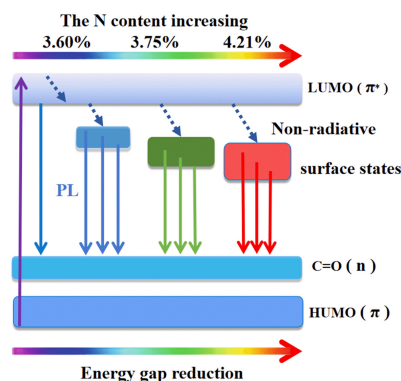


Figure 7. The sketch diagram of color tuning mechanism in N-CNDs.

4. Conclusions

In conclusion, we have prepared N-CNDs by microwave method with citric acid and L-glutamic acid as carbon source, and deionized water as a dispersing agent. The optical properties of different N-doping CNDs have been investigated with different ratios between citric acid and L-glutamic acid. The results indicate that many functional groups, such as C-O, C=O, C-O-C, C-N attached to the surface/edges of carbon nucleus of N-CNDs, exist. The prepared N-CNDs with the ratios of the raw materials at 1:1, 1:2, and 1:3 can emit blue (445 nm), green (546 nm), and orange (617 nm) fluorescence, respectively. Different N concentrations doped into N-CNDs can lead to different surface/edge states, and the wavelength of the PL emission from N-CNDs can be tuned via controlling the N concentration in CNDs. The PL intensity of N-CNDs is associated with the content of C-O groups on the surface/edges of N-CNDs. The wavelength of the PL emission from N-CNDs shows a red-shift, with increasing of the N concentration in N-CNDs. The interesting and important findings from this study can help us to gain a better understanding of the microscopic mechanism for achieving multi-colour fluorescent CNDs.

Author Contributions: W.L. and J.T. prepared the samples and carried out the experimental measurements. Y.L., H.B. and W.Z. participated in the sample preparation and the analyses of the experimental results. J.Z. proposed the research work, designed the experiments and prepared the manuscript. Y.X. and W.X. participated in the analyses of the experimental results and the preparation of the manuscript. All authors read and approved the final manuscript.

Funding: This work was supported by the National Natural Science Foundation of China (grant Nos. 12064049, 11664044, U1930116, U1832153, U206720039, 12004331, 11847054), the Department of Science and Technology of Yunnan Province (grant Nos. 202004AP080053, 2019FD134), Shenzhen Science and Technology Program (KQTD20190929173954826).

Conflicts of Interest: The authors declare no conflict of interest.

References

1. Xu, X.; Ray, R.; Gu, Y.; Ploehn, H.J.; Gearheart, L.; Raker, K.; Scrivens, W.A. Electrophoretic analysis and purification of fluorescent single-walled carbon nanotube fragments. *J. Am. Chem. Soc.* **2004**, *126*, 12736–12737.
2. Li, H.; Kang, Z.; Liu, Y.; Lee, S. Carbon nanodots: Synthesis, properties and applications. *J. Mater. Chem.* **2012**, *22*, 24230.
3. Zhu, S.; Song, Y.; Zhao, X.; Shao, J.; Zhang, J.; Yang, B. The photoluminescence mechanism in carbon dots (graphene quantum dots, carbon nanodots, and polymer dots): Current state and future perspective. *Nano Res.* **2015**, *8*, 355–381. [[CrossRef](#)] [[PubMed](#)]

4. Sun, Y.; Zhou, B.; Lin, Y.; Wang, W.; Fernando, K.S.; Pathak, P.; Meziani, M.J.; Harruff, B.A.; Wang, X.; Wang, H.; et al. Quantum-sized carbon dots for bright and colorful photoluminescence. *J. Am. Chem. Soc.* **2006**, *128*, 7756–7757. [[CrossRef](#)] [[PubMed](#)]
5. Zhao, J.; Luo, Q.; Ruan, Q.; Chen, K.; Liu, C.; Redshaw, C.; Jin, Z. Red/Green Tunable-Emission Carbon Nanodots for Smart Visual Precision pH Sensing. *Chem. Mater.* **2021**, *33*, 6091–6098. [[CrossRef](#)] [[PubMed](#)]
6. Liu, J.; Geng, Y.; Li, D.; Yao, H.; Huo, Z.; Li, Y.; Zhang, K.; Zhu, S.; Wei, H.; Xu, W.; et al. Deep Red Emissive Carbonized Polymer Dots with Unprecedented Narrow Full Width at Half Maximum. *Adv. Mater.* **2020**, *32*, 1906641. [[CrossRef](#)] [[PubMed](#)]
7. Wu, Z.L.; Gao, M.X.; Wang, T.T.; Wan, X.Y.; Zheng, L.L.; Huang, C.Z. A general quantitative pH sensor developed with dicyandiamide N-doped high quantum yield graphene quantum dots. *Nanoscale* **2014**, *6*, 3868–3874. [[CrossRef](#)]
8. Qian, Z.; Ma, J.; Shan, X.; Feng, H.; Shao, L.; Chen, J. Highly luminescent N-Doped carbon quantum dots as an effective multifunctional fluorescence sensing platform. *Chem. Eur. J.* **2014**, *20*, 2254–2263. [[CrossRef](#)]
9. Li, X.; Zhang, S.; Kulinich, S.A.; Liu, Y.; Zeng, H. Engineering surface states of carbon dots to achieve controllable luminescence for solid-luminescent composites and sensitive Be^{2+} detection. *Sci. Rep.* **2014**, *4*, 4976. [[CrossRef](#)]
10. Hu, Y.; Yang, Z.; Lu, X.; Guo, J.; Cheng, R.; Zhu, L.; Wang, C.; Chen, S. Facile Synthesis of Red Dual-emissive Carbon Dots for Ratiometric Fluorescence Sensing and Cellular Imaging. *Nanoscale* **2020**, *12*, 5494–5500. [[CrossRef](#)]
11. Shen, L.; Zhang, L.; Chen, M.; Chen, X.; Wang, J. The production of pH-sensitive photoluminescent carbon nanoparticles by the carbonization of polyethylenimine and their use for bioimaging. *Carbon* **2013**, *55*, 343–349. [[CrossRef](#)]
12. Zhu, S.; Zhang, J.; Qiao, C.; Tang, S.; Li, Y.; Yuan, W.; Li, B.; Tian, L.; Liu, F.; Hu, R.; et al. Strongly green photoluminescent graphene quantum dots for bioimaging applications. *Chem. Commun.* **2011**, *47*, 6858–6860. [[CrossRef](#)]
13. Pan, D.; Zhang, J.; Li, Z.; Wu, C.; Yan, X.; Wu, M. Observation of pH-, solvent-, spin-, and excitation-dependent blue photoluminescence from carbon nanoparticles. *Chem. Commun.* **2010**, *46*, 3681–3683. [[CrossRef](#)] [[PubMed](#)]
14. Kozák, O.; Datta, K.K.R.; Greplová, M.; Ranc, V.; Kašlík, J.; Zbořil, R. Surfactant derived amphiphilic carbon dots with tunable photoluminescence. *Phys. Chem. C* **2013**, *117*, 24991–24996. [[CrossRef](#)]
15. Li, D.; Hu, X.; Li, Q.; Dong, L.; Huang, J.; Li, H.; Xie, H.; Xiong, C. Self-assembled long-chain organic ion grafted carbon dot ionic nanohybrids with liquid-like behavior and dual luminescence. *N. J. Chem.* **2013**, *37*, 3857–3860. [[CrossRef](#)]
16. Liu, S.-S.; Wang, C.-F.; Li, C.-X.; Wang, J.; Mao, L.-H.; Chen, S. Hair-derived carbon dots toward versatile multidimensional fluorescent materials. *J. Mater. Chem. C* **2014**, *2*, 6477–6483. [[CrossRef](#)]
17. Dong, Y.; Cai, J.; Fang, Q.; You, X.; Chi, Y. Dual-emission of lanthanide metal organic frameworks encapsulating carbon-based dots for ratio metric detection of water in organic solvents. *Anal. Chem.* **2016**, *88*, 1748–1752. [[CrossRef](#)]
18. Wang, T.-Y.; Chen, C.-Y.; Wang, C.-M.; Tan, Y.Z.; Liao, W.-S. Multicolor functional carbon dots via one-step refluxing synthesis. *ACS Sens.* **2017**, *2*, 354–363. [[CrossRef](#)]
19. Bhunia, S.K.; Saha, A.; Maity, A.R.; Ray, S.C.; Jana, N.R. Carbon nanoparticle based fluorescent bioimaging probes. *Sci. Rep.* **2013**, *3*, 1473. [[CrossRef](#)]
20. Purbia, R.; Paria, S. A simple turn on fluorescent sensor for the selective detection of thiamine using coconut water derived luminescent carbon dots. *Biosens. Bioelectron.* **2016**, *79*, 467–475. [[CrossRef](#)]
21. Xiao, S.J.; Chu, Z.J.; Zuo, J.; Zhao, X.J.; Huang, C.Z.; Zhang, L. Fluorescent carbon dots: Facile synthesis at room temperature and its application for Fe^{2+} sensing. *J. Nanopart. Res.* **2017**, *19*, 84. [[CrossRef](#)]
22. Yogesh, G.K.; Shuaib, E.P.; Sastikumar, D. Photoluminescence properties of carbon nanoparticles synthesized from activated carbon powder (4% ash) by laser ablation in solution. *Mater. Res. Bull.* **2017**, *91*, 220–226. [[CrossRef](#)]
23. Sun, D.; Ban, R.; Zhang, P.-H.; Wu, G.-H.; Zhang, J.-R.; Zhu, J.-J. Hair fiber as a precursor for synthesizing of sulfur-and nitrogen-co-doped carbon dots with tunable luminescence properties. *Carbon* **2013**, *64*, 424–434. [[CrossRef](#)]
24. Van Khai, T.; Na, H.G.; Kwak, D.S.; Kwon, Y.J.; Ham, H.; Shim, K.B.; Kim, H.W. Influence of N-doping on the structural and photoluminescence properties of graphene oxide films. *Carbon* **2012**, *50*, 3799–3806. [[CrossRef](#)]

25. Shi, L.; Li, Y.; Li, X.; Zhao, B.; Wen, X.; Zhang, G.; Dong, C.; Shuang, S. Controllable synthesis of green and blue fluorescent carbon nanodots for pH and Cu^{2+} sensing in living cells. *Biosens. Bioelectron.* **2016**, *77*, 598–602. [[CrossRef](#)]
26. Kunderlev, E.V.; Teplakov, N.V.; Leonov, M.Y.; Maslov, V.G.; Baranov, A.V.; Fedorov, A.V.; Rukhlenko, I.D.; Rogach, A.L. Amino Functionalization of Carbon Dots Leads to Red Emission Enhancement. *J. Phys. Chem. Lett.* **2019**, *10*, 5111–5116. [[CrossRef](#)]
27. Miao, X.; Qu, D.; Yang, D.; Nie, B.; Zhao, Y.; Fan, H.; Sun, Z. Synthesis of Carbon Dots with Multiple Color Emission by Controlled Graphitization and Surface Functionalization. *Adv. Mater.* **2018**, *30*, 1704740. [[CrossRef](#)]
28. Guo, L.; Ge, J.; Liu, W.; Niu, G.; Jia, Q.; Wang, H.; Wang, P. Tunable multicolor carbon dots prepared from well-defined polythiophene derivatives and their emission mechanism. *Nanoscale* **2016**, *8*, 729–734. [[CrossRef](#)]
29. Zhang, J.; Wang, H.; Xiao, Y.; Tang, J.; Liang, C.; Li, F.; Dong, H.; Xu, W. A Simple Approach for Synthesizing of Fluorescent Carbon Quantum Dots from Tofu Wastewater. *Nanoscale Res. Lett.* **2017**, *12*, 611. [[CrossRef](#)]
30. Bao, L.; Liu, C.; Zhang, Z.-L.; Pang, D.-W. Photoluminescence-Tunable Carbon Nanodots: Surface-State Energy-Gap Tuning. *Adv. Mater.* **2015**, *27*, 1663–1667. [[CrossRef](#)]
31. Jiang, K.; Sun, S.; Zhang, L.; Lu, Y.; Wu, A.; Cai, C.; Lin, H. Red, Green, and Blue Luminescence by Carbon Dots: Full-Color Emission Tuning and Multicolor Cellular Imaging. *Adv. Mater.* **2015**, *54*, 5360–5363. [[CrossRef](#)]
32. Xu, Y.; Wu, M.; Liu, Y.; Feng, X.-Z.; Yin, X.-B.; He, X.-W.; Zhang, Y.-K. Nitrogen-Doped Carbon Dots: A Facile and General Preparation Method, Photoluminescence Investigation, and Imaging Applications. *Chem. Eur. J.* **2013**, *19*, 2276–2283. [[CrossRef](#)]
33. Han, L.; Liu, S.G.; Dong, J.X.; Liang, J.Y.; Li, L.J.; Li, N.B.; Luo, H.Q. Facile synthesis of multicolor photoluminescent polymer carbon dots with surface-state energy gap-controlled emission. *J. Mater. Chem. C* **2017**, *5*, 10785–10793. [[CrossRef](#)]
34. Yuan, F.; Wang, Z.; Li, X.; Li, Y.; Tan, Z.; Fan, L.; Yang, S. Bright Multicolor Bandgap Fluorescent Carbon Quantum Dots for Electroluminescent Light-Emitting Diodes. *Adv. Mater.* **2016**, *29*, 1604436. [[CrossRef](#)]
35. Ding, H.; Yu, S.-B.; Wei, J.-S.; Xiong, H.-M. Full-Color Light-Emitting Carbon Dots with a Surface-State-Controlled Luminescence Mechanism. *ACS Nano* **2015**, *10*, 484–491. [[CrossRef](#)]
36. Zhu, S.; Shao, J.; Song, Y.; Zhao, X.; Du, J.; Wang, L.; Wang, H.; Zhang, K.; Zhang, J.; Yang, B. Investigating the surface state of graphene quantum dots. *Nanoscale* **2015**, *7*, 7, 7927–7933. [[CrossRef](#)]
37. Zhang, Y.; Liu, X.; Fan, Y.; Guo, X.; Zhou, L.; Lv, Y.; Lin, J. One-Step Microwave Synthesis of N-Doped Hydroxyl-Functionalized Carbon Dots with Ultra-High Fluorescence Quantum Yields. *Nanoscale* **2016**, *8*, 15281–15287. [[CrossRef](#)]
38. Tang, J.; Zhang, J.; Zhang, W.; Xiao, Y.; Shi, Y.; Kong, F.; Xu, W. Modulation of red-light emission from carbon quantum dots in acid-base environment and the detection of Chromium (III) ions. *J. Mater. Sci. Technol.* **2021**, *83*, 58–65. [[CrossRef](#)]
39. Omer, K.M.; Hassan, A.Q. Chelation-enhanced fluorescence of phosphorus doped carbon nanodots for multi-ion detection. *Microchim. Acta* **2017**, *184*, 2063–2071. [[CrossRef](#)]

40. Hu, S.; Trinchì, A.; Atkin, P.; Cole, I. Tunable photoluminescence across the entire visible spectrum from carbon dots excited by white light. *Angew. Chem. Int. Ed.* **2015**, *54*, 2970–29741. [[CrossRef](#)]
41. Tucureanu, V.; Matei, A.; Avram, A.M. FTIR Spectroscopy for Carbon Family Study. *Crit. Rev. Anal. Chem.* **2016**, *46*, 502–520. [[CrossRef](#)]

© 2021 by the authors. Submitted to *Nanomaterials* for possible open access publication under the terms and conditions of the Creative Commons Attribution (CC BY) license (<http://creativecommons.org/licenses/by/4.0/>).